

Real-time automotive slip angle estimation with extended H_∞ circle criterion observer for nonlinear output system

Gridsada Phanomchoeng, Ali Zemouche, Rajesh Rajamani

▶ **To cite this version:**

Gridsada Phanomchoeng, Ali Zemouche, Rajesh Rajamani. Real-time automotive slip angle estimation with extended H_∞ circle criterion observer for nonlinear output system. American Control Conference, ACC 2017, May 2017, Seattle, WA, United States. 10.23919/acc.2017.7963187 . hal-01541110

HAL Id: hal-01541110
https://hal.science/hal-01541110

Submitted on 12 Jan 2018

HAL is a multi-disciplinary open access archive for the deposit and dissemination of scientific research documents, whether they are published or not. The documents may come from teaching and research institutions in France or abroad, or from public or private research centers.

L'archive ouverte pluridisciplinaire **HAL**, est destinée au dépôt et à la diffusion de documents scientifiques de niveau recherche, publiés ou non, émanant des établissements d'enseignement et de recherche français ou étrangers, des laboratoires publics ou privés.

Real-Time Automotive Slip Angle Estimation with Extended H_∞ Circle Criterion Observer for Nonlinear Output System

G. Phanomchoeng[1], A. Zemouche[2], and R. Rajamani[3]

***Abstract*— Many active vehicle safety systems such as electronic stability control (ESC), rollover prevention, and lane departure avoidance could benefit from knowledge of the vehicle slip angle. However, it is a challenge to design an observer to estimate slip angle reliably under a wide range of vehicle maneuvers and operating conditions. This is due especially to nonlinear tire characteristics and system models which have nonlinear output equations. Hence this paper develops an extended H_∞ circle criterion observer for state estimation in systems with nonlinear output equations. The observer design approach utilizes a modified Young's relation to include additional degrees of freedom in the linear matrix inequality (LMI) used for observer gain design. This enhanced LMI is less conservative than others proposed in the literature for Lipschitz nonlinear systems, both with and without nonlinear output equations. The observer is applied to slip angle estimation and utilizes inexpensive sensors available in all modern vehicles. Finally, experimental tests on a Volvo XC90 sport utility vehicle are used to evaluate the developed approach. The experimental results show that the slip angle estimates for a variety of test maneuvers on road surfaces with different friction coefficients are reliable.**

***Index Terms* — Slip angle estimation, Lipschitz system, LMI approach, H_∞ synthesis, nonlinear observer design, electronic stability control (ESC).**

I. Introduction

Over 94% of traffic accidents are found to be related to human error [1]. Active safety control systems can help reduce driver burden, partially automate normal driving operations, and reduce accidents. Many driver assistance systems such as electronic stability control (ESC) [2, 3], rollover prevention [4], lane departure avoidance systems [5], collision avoidance systems [6], and adaptive cruise control (ACC) systems have been developed in the last ten years [2].

It is predicted that ESC systems can reduce single-vehicle crashes of passenger cars by 34 percent and single-vehicle crashes of sport utility vehicles (SUVs) by 59 percent, with a much greater drop in rollover crashes. Hence, ESC systems are now mandated in all new vehicles from 2012 [7].

Many electronic stability control systems focus on yaw rate feedback for enhancing vehicle stability performance. However, it is beneficial to also control the vehicle slip angle besides controlling yaw rate, especially in loss of stability situations on low-friction road surfaces [3, 8]. The slip angle feedback is necessary since too large a value of it can reduce the ability of the tires to generate lateral forces and reduce the stability control performance of the system. Thus, both yaw rate and vehicle slip angle are variables needed for vehicle stability control.

The yaw rate signal can be measured by an inexpensive gyroscope sensor. However, the slip angle cannot be easily measured with inexpensive sensors. Further, estimation of the slip angle is also a challenge due to the nonlinearity of the lateral dynamics during loss of stability control situations. Therefore, this paper focuses on slip angle estimation using a nonlinear observer, namely an extended H_∞ circle criterion observer for nonlinear systems with nonlinear output equations. The observer presented here is an extension of the theoretical observer design result presented in [9] for nonlinear systems with linear outputs.

The outline of the paper is as follows. Section 2 presents a review of slip angle estimation methods. Then, the notations and preliminaries are presented in Section 3 and the development of the extended H_∞ circle criterion observer for nonlinear output systems is presented in Section 4. Next, Section 5 applies the developed observer to estimate vehicle slip angle. The experimental setup and results are presented in Section 6 and Section 7 respectively. Finally, the conclusions are presented in Section 8.

II. Review of Slip Angle Estimation Methods

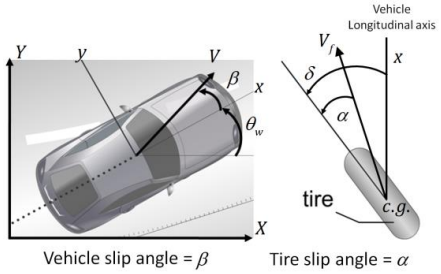


Figure 1 Vehicle and tire slip angles.

The slip angle of a vehicle β is the angle which its velocity vector at the center of gravity (c.g.) makes with the longitudinal axis of the vehicle. The slip angle of a tire α is the angle of the velocity vector at the tire with the orientation of the tire [2]. Both of these definitions are illustrated in Figure 1.

[1]G. Phanomchoeng is with the Department of Mechanical Engineering, Chulalongkorn University, Bangkok, 10330, Thailand, Email: gridsada.p@chula.ac.th

[2]A. Zemouche is with University of Lorraine, CRAN CNRS UMR 7039, 54400 Cosnes et Romain, France, Email: ali.zemouche@univ-lorraine.fr and with EPI INRIA DISCO, Laboratoire des Signaux et Systèmes, CNRS-Supélec, 91192 Gif-sur-Yvette, France, Email: ali.zemouche@inria.fr

[3]R. Rajamani is with Laboratory for Innovations in Sensing, Estimation, and Control, Department of Mechanical Engineering, University of Minnesota, Minneapolis, USA, Email: rajamani@me.umn.edu

A. Slip Angle Measurement Sensors

The global position of the vehicle can be measured by a one-antenna GPS system. However, this system cannot measure slip angle. As a result, many researchers have attempted to estimate slip angle by using an integrated estimation algorithm that combines an inertial measurement unit and a one-antenna GPS system [10]. However, the drift in the velocity estimates due to bias errors in the acceleration measurements continues to be a major problem of this integration approach. Another problem of the GPS-based system is the occasional unavailability of the GPS satellite signal, especially in urban areas and areas covered with tall buildings. To correct the bias errors and to obtain absolute orientation of the vehicle, a two-antenna GPS system can be used [11]. However, this system is costly, with an approximate cost of at least $600 for sedans [12].

B. Dynamic Model-Based Estimation

Slip angle estimation using an observer is inexpensive compared to a GPS-based system and compared to optical sensors. The slip angle estimation system can utilize sensors already being used by the vehicle stability control system. Several slip angle estimation approaches have been developed, which can be categorized into two groups: kinematics-based methods [12] and vehicle-model-based methods [3]. The kinematics-based approaches are very sensitive to sensor error, particularly sensor bias error, which causes a drift. The vehicle-model-based methods are relatively robust against sensor bias errors. However, they rely on the accuracy of the vehicle model, vehicle parameters and tire parameters and knowledge of road conditions. Also, most of the observer-based slip angle estimation methods published in literature rely on linear vehicle models. Therefore, when the vehicle is skidding and the slip angle becomes large, these estimation methods will *not* be reliable.

In this paper, a newly developed H_∞ observer is used to estimate the vehicle slip angle based on a nonlinear vehicle model with output nonlinear equations. The observer can work well for a large range of operating conditions and friction coefficient ranges. The developed technique is validated with experimental measurements on a test vehicle, a Volvo XC90 sport utility vehicle.

III. Notations and Preliminaries

Notations: Throughout the paper, the following notations are used:

- (*) is used for the blocks induced by symmetry;
- $\mathbb{I}_r$ represents the identity matrix of dimension r;
- For a square matrix S, $S > 0$ ($S < 0$) means that this matrix is positive definite (negative definite);
- $e_s(i) = \underbrace{\left[0, \dots, 0, \overset{i\,th}{\overbrace{1}}, 0, \dots, 0\right]^T}_{s\ components} \in \mathbb{R}^s$, $s \geq 1$ is a vector of the canonical basis of $\mathbb{R}^s$.

Preliminaries:

Lemma 1 ([13]) Consider two vectors

$$X = \begin{bmatrix} x_1 \\ \vdots \\ x_n \end{bmatrix} \in \mathbb{R}^n \text{ and } Y = \begin{bmatrix} y_1 \\ \vdots \\ y_n \end{bmatrix} \in \mathbb{R}^n. \quad (1)$$

For all $i = 0, \dots, n$, an auxiliary vector $X^{Y_i} \in \mathbb{R}^n$ corresponding to X and Y can be defined as follows:

$$\begin{cases} X^{Y_i} = \begin{bmatrix} y_1 \\ \vdots \\ y_i \\ x_{i+1} \\ \vdots \\ x_n \end{bmatrix} for\ i = 1, \dots, n \\ X^{Y_0} = X \end{cases} \quad (2)$$

Lemma 2 ([13]) Consider a function Ψ: $\mathbb{R}^n \to \mathbb{R}^n$. Then, the two following items are equivalent:

Ψ is globally Lipschitz with respect to its argument, i.e.:

$$\|\Psi(X) - \Psi(Y)\| \leq \gamma_\Psi \|X - Y\|, \quad \forall X, Y \in \mathbb{R}^n \quad (3)$$

for all $i, j = 1, \dots, n$, there exist functions

$$\Psi_{ij}: \mathbb{R}^n \times \mathbb{R}^n \to \mathbb{R} \quad (4)$$

and constants $\underline{\gamma}_{\Psi_{ij}}$ and $\overline{\gamma}_{\Psi_{ij}}$, so that $\forall X, Y \in \mathbb{R}^n$,

$$\Psi(X) - \Psi(Y) = \sum_{i=1}^{i=n} \sum_{j=1}^{j=n} \psi_{ij} \mathcal{H}_{ij} (X - Y) \quad (5)$$

and

$$\underline{\gamma}_{\psi_{ij}} \leq \psi_{ij} \leq \overline{\gamma}_{\psi_{ij}} \quad (6)$$

where

$$\psi_{ij} \triangleq \psi_{ij}(X^{Y_{j-1}}, X^{Y_j}) \text{ and } \mathcal{H}_{ij} = e_n(i) e_n^T(j). \quad (7)$$

PROOF: The proof is omitted. See [13].

Lemma 3 (Reformulation of Young's relation [11]) Let X and Y two given matrices of appropriate dimensions. Then, for any symmetric positive definite matrix S of appropriate dimension, the following inequality holds:

$$X^T Y + Y^T X \leq \frac{1}{2} [X + SY]^T S^{-1} [X + SY]. \quad (8)$$

PROOF. The proof is omitted. See [9].

IV. Extended H_∞ Observer for Nonlinear Output System

3.1 Problem Statement

A nonlinear dynamic system with nonlinear outputs is often encountered in many real applications, such as the problem of magnetic position estimation [14] and slip angle estimation problems [3]. Consider the class of nonlinear systems described by:

$$\begin{aligned} \dot{x} &= Ax + G\gamma(x) + E\omega \\ y &= Cx + Bg(x) + D\omega \end{aligned} \quad (9)$$

where $x \in \mathbb{R}^n$ is the state vector, $y \in \mathbb{R}^p$ is the output measurement vector, and $\omega \in \mathbb{R}^q$ is the disturbance $\mathcal{L}_2$ bounded vector. $A \in \mathbb{R}^{n \times n}$, $G \in \mathbb{R}^{n \times m}$, $E \in \mathbb{R}^{n \times q}$, $C \in \mathbb{R}^{p \times n}$, $B \in \mathbb{R}^{p \times s}$, and $D \in \mathbb{R}^{p \times q}$ are appropriate matrices. The functions $\gamma(x)$: $\mathbb{R}^n \to \mathbb{R}^m$ and $g(x)$: $\mathbb{R}^n \to \mathbb{R}^s$ are nonlinear and assumed to be globally Lipschitz.

$\gamma(x)$ and $g(x)$ can be written under the detailed form:

$$\gamma(x) = \begin{bmatrix} \gamma_1(H_1 x) \\ \vdots \\ \overset{\nu_i}{\overbrace{\gamma_i(H_i x)}} \\ \vdots \\ \gamma_m(H_m x) \end{bmatrix}, \quad g(x) = \begin{bmatrix} g_1(F_1 x) \\ \vdots \\ \overset{\theta_i}{\overbrace{g_i(F_i x)}} \\ \vdots \\ g_s(F_s x) \end{bmatrix} \quad (10)$$

where $H_i \in \mathbb{R}^{n_i \times n}$ and $F_i \in \mathbb{R}^{p_i \times n}$.

3.2 Observer Design

The observer is than assumed to be of the generalized Arcak's observer form as follows:

$$\dot{\hat{x}} = A\hat{x} + G[\gamma_1(\hat{\mathcal{v}}_1) \quad \cdots \quad \gamma_i(\hat{\mathcal{v}}_i) \quad \cdots \quad \gamma_m(\hat{\mathcal{v}}_m)]^T + L(y - \hat{y}) \tag{11a}$$

$$\hat{y} = C\hat{x} + B\left[g_1(\hat{\theta}_1) \quad \cdots \quad g_i(\hat{\theta}_i) \quad \cdots \quad g_s(\hat{\theta}_s)\right]^T \tag{11b}$$

$$\hat{\mathcal{v}}_i = H_i\hat{x} + K_i(y - \hat{y}) \tag{11c}$$

$$\hat{\theta}_i = F_i\hat{x} + M_i(y - z) \tag{11d}$$

$$z = C\hat{x} + B[g_1(F_1\hat{x}) \quad \cdots \quad g_i(F_i\hat{x}) \quad \cdots \quad g_s(F_s\hat{x})]^T \tag{11e}$$

The matrices $L \in \mathbb{R}^{n \times p}$, $K_i \in \mathbb{R}^{n_i \times p}$, and $M_i \in \mathbb{R}^{p_i \times p}$ are to be determined so that the estimation error $e = x - \hat{x}$ converges asymptotically towards zero.

Since $\gamma(.)$ and $g(.)$ are globally Lipschitz, then from Lemma 2 there exist functions

$$\phi_{ij}: \mathbb{R}^{n_i} \times \mathbb{R}^{n_i} \to \mathbb{R}\,, \psi_{ij}: \mathbb{R}^{p_i} \times \mathbb{R}^{p_i} \to \mathbb{R} \tag{12}$$

and constants a_{ij}, b_{ij}, c_{ij}, and d_{ij}, such that

$$\begin{aligned} \gamma(x) - \gamma(\hat{x}) &= \textstyle\sum_{i,j=1}^{i,j=m,n_i} \phi_{ij}\mathcal{H}_{ij}(\mathcal{v}_i - \hat{\mathcal{v}}_i), \\ g(x) - g(\hat{x}) &= \textstyle\sum_{i,j=1}^{i,j=q,p_i} \psi_{ij}\mathcal{F}_{ij}\left(\theta_i - \hat{\theta}_i\right) \end{aligned} \tag{13}$$

with

$$\begin{aligned} a_{ij} \le \phi_{ij}\left(\mathcal{v}_i^{\hat{\mathcal{v}}_{i,j-1}}, \mathcal{v}_i^{\hat{\mathcal{v}}_{i,j}}\right) \le b_{ij}, \\ c_{ij} \le \psi_{ij}\left(\theta_i^{\hat{\theta}_{i,j-1}}, \theta_i^{\hat{\theta}_{i,j}}\right) \le d_{ij}. \end{aligned} \tag{14}$$

For shortness, it can set

$$\begin{aligned} \phi_{ij} \triangleq \phi_{ij}\left(\mathcal{v}^{\hat{\mathcal{v}}_{i,j-1}}, \mathcal{v}^{\hat{\mathcal{v}}_{i,j}}\right), \psi_{ij} \triangleq \\ \psi_{ij}\left(\theta_i^{\hat{\theta}_{i,j-1}}, \theta_i^{\hat{\theta}_{i,j}}\right). \end{aligned} \tag{15}$$

Without loss of generality, it can assume that $a_{ij} = 0$ for all $j = 1, \dots, n_i$ and $i = 1, \dots, m$ and $c_{ij} = 0$, for $i = 1, \dots, q_i$ and $i = 1, \dots, q$. The detail of these is presented in [15].

Since $\mathcal{v}_i - \hat{\mathcal{v}}_i = (H_i - K_iC)e - K_iD\omega$ and $\theta_i - \hat{\theta}_i = (F_i - M_iC)e - M_iD\omega$, then

$$\begin{aligned} \gamma(x) - \gamma(\hat{x}) &= \left[\sum_{i,j=1}^{i,j=m,n_i} \phi_{ij}\mathcal{H}_{ij}(H_i - K_iC)\right]e \\ &\quad - \left[\sum_{i,j=1}^{i,j=m,n_i} \phi_{ij}\mathcal{H}_{ij}K_iD\right]\omega, \\ g(x) - g(\hat{x}) &= \left[\sum_{i,j=1}^{i,j=q,p_i} \psi_{ij}\mathcal{F}_{ij}(F_i - M_iC)\right]e \\ &\quad - \left[\sum_{i,j=1}^{i,j=q,p_i} \psi_{ij}\mathcal{F}_{ij}M_iD\right]\omega. \end{aligned} \tag{16}$$

Consequently, the dynamics equation of the estimation error is then given by:

$$\begin{aligned} \dot{e} = &\left(\mathbb{A}_L + \sum_{i,j=1}^{i,j=m,n_i}\left[\phi_{ij}G\mathcal{H}_{ij}\mathbb{H}_{K_i}\right]\right)e + \left[\sum_{i,j=1}^{i,j=q,p_i}\psi_{ij}LB\mathcal{F}_{ij}\mathbb{F}_{M_i}\right]e \\ &+\left(\mathbb{E}_L + \sum_{i,j=1}^{i,j=m,n_i}\left[\phi_{ij}G\mathcal{H}_{ij}\mathbb{D}_{K_i}\right]\right)\omega + \left[\sum_{i,j=1}^{i,j=q,p_i}\psi_{ij}LB\mathcal{F}_{ij}\mathbb{D}_{M_i}\right]\omega \end{aligned} \tag{17}$$

where

$$\mathbb{A}_L = A - LC, \mathbb{E}_L = E - LD \tag{18}$$

$$\mathbb{H}_{K_i} = H_i - K_iC, \mathbb{D}_{K_i} = -K_iD$$

$$\mathbb{F}_{M_i} = -(F_i - M_iC), \mathbb{D}_{M_i} = M_iD.$$

The aim consists in finding the gains L, K_i for $i = 1, \dots, m$, and M_i for $i = 1, \dots, q$ so that the estimation error dynamics equation (17) turn to be $\mathcal{H}_\infty$ asymptotically stable. That is, the objective is to determine the observer parameters such that the following $\mathcal{H}_\infty$ criterion is satisfied:

$$\|e\|_{\mathcal{L}_2^n} \le \sqrt{\mu\|\omega\|_{\mathcal{L}_2^q}^2 + \mathcal{V}\|e_0\|^2} \tag{19}$$

where $\mu > 0$ is the disturbance attenuation level and $\mathcal{V} > 0$ is to be determined. To be more clear, $\sqrt{\mu}$ is the disturbance gain from ω to e.

As usual for this class of systems addressed by LMI techniques, we use a quadratic Lyapunov function to analyze the $\mathcal{H}_\infty$ stability. That is

$$V(e) = e^T\mathbb{P}e, \ \mathbb{P} = \mathbb{P}^T > 0 \tag{20}$$

Consequently, $\mathcal{H}_\infty$ criterion equation (19) is satisfied if the following inequality holds [17]:

$$\mathcal{W} \triangleq \dot{V}(e) + \|e\|^2 - \mu\|\omega\|^2 \le 0. \tag{21}$$

This problem has been handled in the literature and several methods have been proposed where each newer method provides relaxed LMI condition. It turns out that all these techniques still provide restrictive LMI synthesis conditions. Despite all the new ways to improve the existing techniques, the problem of observer design for Lipschitz nonlinear systems remains a challenge to solve. Therefore, an enhanced LMI condition, for which the use a diagonal form of the multiplier matrix is not required, is proposed.

Then, by using Lemma 3 and some mathematical manipulation, the following Theorem 1 for the nonlinear observer can be developed.

Theorem 1 Assume that there exist symmetric positive definite matrices $\mathbb{P} \in \mathbb{R}^{n \times n}$, $\mathcal{Z}_i \in \mathbb{R}^{n_i \times n_i}$, $\mathcal{S}_i \in \mathbb{R}^{p_i \times p_i}$, and matrices $\mathcal{R} \in \mathbb{R}^{p \times n}$, $\mathcal{T}_i \in \mathbb{R}^{p \times n_i}$, $\bar{\mathcal{T}}_i \in \mathbb{R}^{p \times p_i}$ of appropriate dimensions so that the following convex optimization problem is solvable:

$$\min(\mu) \ subject \ to \ (23) \tag{22}$$

$$\begin{bmatrix} \mathbb{A}(\mathbb{P},\mathcal{R}) & \mathbb{P}E - \mathcal{R}^TD & \overbrace{[\Sigma_1 \dots \Sigma_m]} & \mathbb{OUT}_{13} \\ (*) & -\mu\mathbb{I}_q & & \\ & (*) & -\wedge\mathbb{Z} & 0 \\ & (*) & (*) & \mathbb{OUT}_{33} \end{bmatrix} \le 0 \tag{23}$$

with

$$\mathbb{A}(\mathbb{P},\mathcal{R}) = A^T\mathbb{P} + \mathbb{P}A - C^T\mathcal{R} - \mathcal{R}^TC + \mathbb{I}_n \tag{24}$$

$$\Sigma_i = [\mathcal{N}_1(\mathbb{P},\mathcal{T}_i,\mathcal{Z}_i) \dots \mathcal{N}_{ni}(\mathbb{P},\mathcal{T}_i,\mathcal{Z}_i)] \tag{25}$$

$$\mathcal{N}_j(\mathbb{P},\mathcal{T}_i,\mathcal{Z}_i) = \begin{bmatrix}\mathbb{P}G\mathcal{H}_{ij} \\ 0\end{bmatrix} + \begin{bmatrix}H_i^T\mathcal{Z}_i - C^T\mathcal{T}_i) \\ -D^T\mathcal{T}_i\end{bmatrix} \tag{26}$$

$$\wedge = block\text{-}diag(\wedge_1, \dots, \wedge_m) \tag{27}$$

$$\wedge_i = block\text{-}diag(\tfrac{2}{b_{i1}}\Pi_{n_i}, \dots, \tfrac{2}{b_{in_i}}\Pi_{n_i}) \tag{28}$$

$$\mathbb{Z} = block\text{-}diag(\mathbb{Z}_i, \dots, \mathbb{Z}_m) \tag{29}$$

$$\mathbb{Z}_i = block\text{-}diag(\overbrace{\mathbb{Z}_i, \dots, \mathbb{Z}_i}^{n_i \ times}) \tag{30}$$

$$\mathbb{OUT}_{13} = \left[\bar{\Sigma}_1 \dots \bar{\Sigma}_q\right] \tag{31}$$

$$\mathbb{OUT}_{33} = -\Pi\mathbb{S} \tag{32}$$

$$\bar{\Sigma}_i = \left[\bar{\mathcal{N}}_1(\mathcal{R},\bar{\mathcal{T}}_i,\mathcal{S}_i) \dots \bar{\mathcal{N}}_{pi}(\mathcal{R},\bar{\mathcal{T}}_i,\mathcal{S}_i)\right] \tag{33}$$

$$\bar{\mathcal{N}}_j(\mathcal{R},\bar{\mathcal{T}}_i,\mathcal{S}_i)=\begin{bmatrix}\mathcal{R}^T B\mathcal{F}_{ij}\\ 0\end{bmatrix}+\begin{bmatrix}-(F_i^T\mathcal{S}_i-C^T\bar{\mathcal{T}}_i)\\ D^T\bar{\mathcal{T}}_i\end{bmatrix} \quad (34)$$

$$\Pi = block\text{-}diag(\Pi_1,\dots,\Pi_q) \quad (35)$$

$$\Pi_{\mathrm{i}} = block\text{-}diag(\tfrac{2}{d_{i1}}\Pi_{p_i},\dots,\tfrac{2}{d_{ip_i}}\Pi_{p_i}) \quad (36)$$

$$\mathbb{S} = block\text{-}diag(\mathbb{S}_i,\dots,\mathbb{S}_q) \quad (37)$$

$$\mathbb{S}_i = block\text{-}diag(\overbrace{\mathcal{S}_i,\dots,\mathcal{S}_i}^{p_i\ times}) \quad (38)$$

Then, the $\mathcal{H}_\infty$criterion (19) is satisfied with $\mathcal{V}=\lambda_{max}(\mathbb{P})$. Hence, the observer gains L, K_i, and M_i are computed by

$$L=\mathbb{P}^{-1}\mathcal{R}^T,\ K_i=\mathcal{Z}_i^{-1}\mathcal{T}_i^T,\ M_i=\mathcal{S}_i^{-1}\bar{\mathcal{T}}_i^T \quad (39)$$

PROOF. To make it simple, let assume that there is not nonlinear outputs, $(g(x)=0, B=0)$, in the system for now. Then, the proof is done by following the steps. By calculating the derivative of $V(e)$ along the trajectories of (17), then

$$\begin{aligned}\mathcal{W} &= e^T\Big[\mathbb{I}_n+\mathbb{P}\Big(\mathbb{A}_L+\textstyle\sum_{i,j=1}^{i,j=m,n_i}[\phi_{ij}G\mathcal{H}_{ij}\mathbb{H}_{K_i}]\Big)\\ &+\Big(\mathbb{A}_L+\textstyle\sum_{i,j=1}^{i,j=m,n_i}[\phi_{ij}G\mathcal{H}_{ij}\mathbb{H}_{K_i}]\Big)^T\mathbb{P}\Big]e\\ &+e^T\Big[\mathbb{P}\Big(\mathbb{E}_L+\textstyle\sum_{i,j=1}^{i,j=m,n_i}[\phi_{ij}G\mathcal{H}_{ij}\mathbb{D}_{K_i}]\Big)\\ &+\Big(\mathbb{E}_L+\textstyle\sum_{i,j=1}^{i,j=m,n_i}[\phi_{ij}G\mathcal{H}_{ij}\mathbb{D}_{K_i}]\Big)^T\mathbb{P}\Big]\omega-\mu\omega^T\omega.\end{aligned} \quad (40)$$

Hence, $\mathcal{W}\le 0$ if the following inequality holds:

$$\overbrace{\begin{bmatrix}\mathbb{A}_L^T\mathbb{P}+\mathbb{P}\mathbb{A}_L+\mathbb{I}_n & \mathbb{P}\mathbb{E}_L\\ \mathbb{E}_L^T\mathbb{P} & -\mu\mathbb{I}_q\end{bmatrix}}^{\mathbb{LINEAR}}+\sum_{i,j=1}^{i,j=m,n_i}\phi_{ij}\begin{pmatrix}\overbrace{\begin{bmatrix}\mathbb{P}G\mathcal{H}_{ij}\\ 0\end{bmatrix}}^{\mathbb{X}_{ij}^T}\overbrace{[\mathbb{H}_{K_i}\quad \mathbb{D}_{K_i}]}^{\mathbb{Y}_i}+\mathbb{Y}_i^T\mathbb{X}_{ij}\\ \end{pmatrix}\le 0. \quad (41)$$

Now, by applying Lemma 3, all symmetric positive definite matrices $\mathbb{S}_{ij}$ will be

$$\mathbb{X}_{ij}^T\mathbb{Y}_i+\mathbb{Y}_i^T\mathbb{X}_{ij}\le\frac{1}{2}\big(\mathbb{X}_{ij}+\mathbb{S}_{ij}\mathbb{Y}_i\big)^T\mathbb{S}_{ij}^{-1}\overbrace{(\mathbb{X}_{ij}+\mathbb{S}_{ij}\mathbb{Y}_i)}^{\Delta_{ij}} \quad (42)$$

Consequently, form equation (14) and the fact that with loss of generality$a_{ij}=0$, inequality (41) is satisfied if

$$\mathbb{LINEAR}+\sum_{i,j=1}^{i,j=m,n_i}\left(\Delta_{ij}^T\left(\frac{2}{b_{ij}}\mathbb{S}_{ij}\right)^{-1}\Delta_{ij}\right)\le 0. \quad (43)$$

Therefore, from Schur Lemma [16], inequality (43) is equivalent to

$$\begin{bmatrix}\mathbb{LINEAR} & [\Delta_1^T\dots\Delta_m^T]\\ (*) & -\wedge\mathbb{S}\end{bmatrix}\le 0 \quad (44)$$

where

$$\Delta_i=\big[\Delta_{11},\dots,\Delta_{1n_i}\big] \quad (45)$$

and

$$\begin{aligned}\mathbb{S} &= block\text{-}diag(\mathbb{S}_1,\dots,\mathbb{S}_m),\\ \mathbb{S}_i &= block\text{-}diag(\mathbb{S}_{i1},\dots,\mathbb{S}_{in_i}).\end{aligned} \quad (46)$$

Regarding the block diagonal form of $\mathbb{Y}_i$, the fact that it does not depend on the index j and depends on the same K_i in the two diagonal blocks, then to obtain an LMI, take $\mathbb{S}=\mathbb{Z}$ as define in equations (29)-(30).

$$\mathbb{S}_{ij}=\mathbb{Z}_i,\forall(i,j) \quad (47)$$

with $\mathbb{Z}_i\in\mathbb{R}^{n_i\times n_i}$. Finally, with the change of variables $\mathcal{R}=L^T\mathbb{P}$ and $\mathcal{T}_i=K_i^T\mathcal{Z}_i$, then the inequality (44) becomes identical to equation (23). Hence, the $\mathcal{H}_\infty$ criterion equation (19) is satisfied with the minimum μ returned by the convex optimization problem (22). This ends the proof of the system without nonlinear outputs. For the system with nonlinear outputs, $\mathcal{W}$ defined in equation (21) is semi-negative definite if the following inequality is fulfilled:

$$\begin{aligned}&\overbrace{\begin{bmatrix}\mathbb{A}_L^T\mathbb{P}+\mathbb{P}\mathbb{A}_L+\mathbb{I}_n & \mathbb{P}\mathbb{E}_L\\ \mathbb{E}_L^T\mathbb{P} & -\mu\mathbb{I}_q\end{bmatrix}}^{\mathbb{LINEAR}}\\ &+\sum_{i,j=1}^{i,j=m,n_i}\phi_{ij}\begin{pmatrix}\overbrace{\begin{bmatrix}\mathbb{P}G\mathcal{H}_{ij}\\ 0\end{bmatrix}}^{\mathbb{X}_{ij}^T}\overbrace{[\mathbb{H}_{K_i}\quad \mathbb{D}_{K_i}]}^{\mathbb{Y}_i}+\mathbb{Y}_i^T\mathbb{X}_{ij}\\ \end{pmatrix}\\ &+\sum_{i,j=1}^{i,j=q,p_i}\psi_{ij}\begin{pmatrix}\overbrace{\begin{bmatrix}\mathbb{P}LB\mathcal{F}_{ij}\\ 0\end{bmatrix}}^{\bar{\mathbb{X}}_{ij}^T}\overbrace{[\mathbb{F}_{M_i}\quad \mathbb{D}_{M_i}]}^{\bar{\mathbb{Y}}_i}+\bar{\mathbb{Y}}_i^T\bar{\mathbb{X}}_{ij}\\ \end{pmatrix}\le\\ &0.\end{aligned} \quad (48)$$

From Schur Lemma [14], the inequalities for all symmetric positive definite matrices $\mathbb{S}_{ij}$ and $\mathbb{M}_{ij}$ is defined by

$$\mathbb{X}_{ij}^T\mathbb{Y}_i+\mathbb{Y}_i^T\mathbb{X}_{ij}\le\frac{1}{2}\big(\mathbb{X}_{ij}+\mathbb{S}_{ij}\mathbb{Y}_i\big)^T\mathbb{S}_{ij}^{-1}\overbrace{(\mathbb{X}_{ij}+\mathbb{S}_{ij}\mathbb{Y}_i)}^{\Delta_{ij}}, \quad (49)$$

$$\bar{\mathbb{X}}_{ij}^T\bar{\mathbb{Y}}_i+\bar{\mathbb{Y}}_i^T\bar{\mathbb{X}}_{ij}\le\frac{1}{2}\big(\bar{\mathbb{X}}_{ij}+\mathbb{M}_{ij}\bar{\mathbb{Y}}_i\big)^T\mathbb{M}_{ij}^{-1}\overbrace{\big(\bar{\mathbb{X}}_{ij}+\mathbb{M}_{ij}\bar{\mathbb{Y}}_i\big)}^{\bar{\Delta}_{ij}}. \quad (50)$$

Then, the proof can be completed by following the proof of the system without nonlinear outputs and shows that the inequality is identical to equation (23).

V. Mathematic Formulation of Slip Angle Estimation Problem

Vehicle Lateral Dynamics

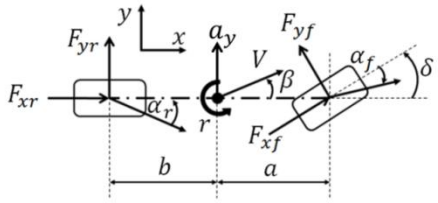


Figure 2 Single track model for vehicle lateral dynamics [3]

The 2 DOF model of the vehicle lateral dynamics as shown in Figure 2 consists of the lateral translation and the yaw rate of the vehicle. The nonlinear vehicle lateral dynamics can be formulated as

$$ma_y=m(\ddot{y}+ru_x)=F_{yf}+F_{yr} \quad (51)$$

$$I_z\dot{r}=aF_{yf}-bF_{yr} \quad (52)$$

where m is the mass of the vehicle, a_y is the lateral acceleration, y is the lateral translation, r is the yaw rate, u_x is the longitudinal velocity, F_{yf} and F_{yr} are the lateral tire forces of the front and rear wheels respectively, I_z is vehicle inertia, and a and b are the distances of the front and rear tires respectively from the c.g. of the vehicle.

The lateral tire force for each of the front and rear tires is calculated from a lateral tire model for parabolic normal pressure distribution [3]:

$$F_y=c_1\alpha-c_2\alpha^2sgn(\alpha)+c_3\alpha^3. \quad (53)$$

where c_1, c_2, and c_3 are the coefficients of the tire form model, and α is the tire slip angle.

The lateral tire forces described by equation (53) are presented in Figure 3.

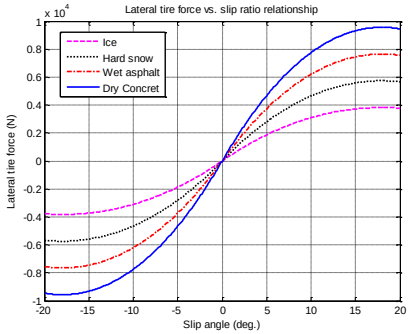


Figure 3 Lateral tire force described by equation (53)

The tire slip angle at the front and rear tires can be related to the body slip angle and the yaw rate using the following linear approximations:

$$\alpha_f = \delta - \left(\beta + \frac{ra}{u_x}\right), \alpha_r = \frac{rb}{u_x} - \beta \tag{54}$$

where α_f and α_r are the tire slip angles of the front and rear wheels respectively, δ is the steering angle, and β is the vehicle slip angle.

The vehicle lateral dynamics equations (51-52) including the nonlinear lateral tire model equation (53) can be rewritten in the standard system dynamics as equation (55).

$$\begin{aligned} \dot{x} &= Ax + \bar{B}u + G\gamma(x) + E\omega \\ y &= Cx + Bg(x) + D\omega \end{aligned} \tag{55}$$

where $\bar{B} \in \mathbb{R}^{n\times d}$ is the matrix, and $u \in \mathbb{R}^d$ is the input vector.

This can be done by choosing the front slip angle α_f and rear slip angle α_r as the state vector. The system equations can be written as

$$\begin{bmatrix}\dot{\alpha}_f \\ \dot{\alpha}_r\end{bmatrix} = \begin{bmatrix} -\left(\frac{u_x}{a+b} + \frac{a^2c_{1f}}{I_z u_x}\right) & \left(\frac{u_x}{a+b} + \frac{abc_{1r}}{I_z u_x}\right) \\ -\left(\frac{u_x}{a+b} - \frac{abc_{1f}}{I_z u_x}\right) & \left(\frac{u_x}{a+b} - \frac{b^2c_{1r}}{I_z u_x}\right) \end{bmatrix}\begin{bmatrix}\alpha_f \\ \alpha_r\end{bmatrix}$$
$$+\begin{bmatrix} \left(\frac{u_x}{a+b}\right) & 1 & -\frac{1}{u_x} \\ \left(\frac{u_x}{a+b}\right) & 0 & -\frac{1}{u_x} \end{bmatrix}\begin{bmatrix}\delta \\ \dot{\delta} \\ a_y\end{bmatrix} + \begin{bmatrix} +\frac{a^2}{I_z u_x} & -\frac{ab}{I_z u_x} \\ -\frac{ab}{I_z u_x} & +\frac{b^2}{I_z u_x} \end{bmatrix}\begin{bmatrix}-\eta(\alpha_f) \\ -\eta(\alpha_r)\end{bmatrix} + \begin{bmatrix}0 \\ 0\end{bmatrix}\omega. \tag{56}$$

where $\eta(\alpha_f) = -c_{2f}\alpha_f^2 sgn(\alpha_f) + c_{3f}\alpha_f^3$, and $\eta(\alpha_r) = -c_{2r}\alpha_r^2 sgn(\alpha_r) + c_{3r}\alpha_r^3$.

The measurement of the system for the observer consists of the lateral acceleration, a_y, and a linear combination of yaw rate , r, and steering angel, δ. The measurement is described by

$$\begin{bmatrix}y_1 \\ y_2\end{bmatrix} = \begin{bmatrix} r - \left(\frac{u_x}{a+b}\right)\delta \\ a_y \end{bmatrix} = \begin{bmatrix} -\left(\frac{u_x}{a+b}\right) & \left(\frac{u_x}{a+b}\right) \\ \frac{c_{1f}}{m} & \frac{c_{1r}}{m} \end{bmatrix}\begin{bmatrix}\alpha_f \\ \alpha_r\end{bmatrix}$$
$$+\begin{bmatrix} 0 & 0 \\ -\frac{1}{m} & -\frac{1}{m} \end{bmatrix}\begin{bmatrix}-\eta(\alpha_f) \\ -\eta(\alpha_r)\end{bmatrix} + \begin{bmatrix}0 \\ 0\end{bmatrix}\omega. \tag{57}$$

Then, the slip angle of the vehicle can be computed from the slip angles of the front and rear tires as

$$\beta = \delta - \left(\alpha_f + \frac{ra}{u_x}\right) \text{ or } \beta = \frac{rb}{u_x} - \alpha_r. \tag{58}$$

Using the LMI toolbox in Matlab, the observer gain based on Theorem 1 are

$$L = \begin{bmatrix} 0.0559 & 0.2677 \\ -0.0471 & 0.3961 \end{bmatrix}, \tag{59}$$
$$K_1 = [-0.0650 \quad 0.0071], K_2 = [0.0650 \quad 0.0071],$$
$$M_1 = [-0.0650 \quad 0.0071], M_2 = [0.0650 \quad 0.0071]$$

VI. Experimental Set Up

The test vehicle used for the experimental evaluation is a Volvo XC90 sport utility vehicle. Vehicle testing was conducted at the Eaton Proving Ground in Marshall, Michigan ([12], [3]). A MicroAutoBox from dSPACE was used for real-time data acquisition. A real-time 6 axis inertial navigation system with combined GPS, RT3000, from Oxford Technical Solutions was used for these tests to accurately measure the vehicle slip angle for comparison with the performance of the slip angle estimation algorithm. The specification of slip angle estimates from this system according to the manufacturer is 0.15 degrees. The GPS outputs were connected to the MicroAutoBox via CAN communication at the baud rate of 0.5 Mbits/sec. To obtain objective test results, the vehicle was instrumented to record the relevant values from both CAN network and GPS. The sampling time is set at 2 ms. A photograph of the test vehicle is shown in Figure 3.



Figure 3 The Volvo XC90 test vehicle with GPS system

VII. Experimental Evaluation of Slip Angle Estimation

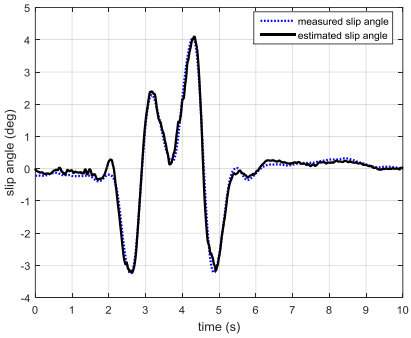


Figure 4 Slip angle estimation result in double lane change test on high friction road surface

Figure 4 and 5 show the experiment results of a double lane change maneuver with vehicle speed at 70 mph and in a random driving maneuver, respectively. The results show that the estimated vehicle slip angle can track the vehicle slip angle obtained from the RT3000 system well. By comparing the results from [3], there is no significate difference between the estimated vehicle slip angles from both observers. However, by looking at the observer gain, L, the observer gain of the $\mathcal{H}_\infty$ observer is lower than that of the bounded Jacobian observer [3]. It means the $\mathcal{H}_\infty$ observer is less conservative than the bounded Jacobian observer. Also, the small gains of the observer will not enhance noise. Another major advantage of the $\mathcal{H}_\infty$ observer over the bounded Jacobian observer is that it is required to solve only one LMI equation for the observer gain.

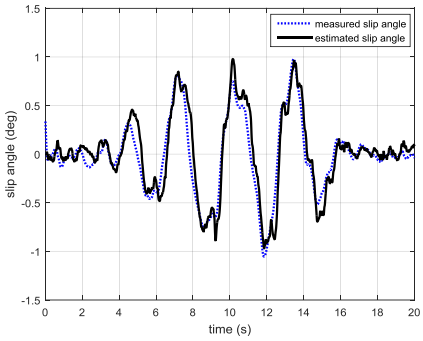


Figure 5 Slip angle estimation result in random driving test

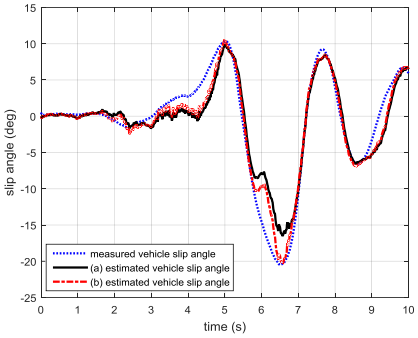


Figure 6 Vehicle slip angle estimation result in double lane change test on low friction coefficient of the road surface (a) the friction coefficient is unknown (b) the friction coefficient is known

Figure 6 show the experimental results of a double lane change test on a low friction coefficient of the road surface. However, the observer gain as obtained from equation (59) is still used for the vehicle slip angle estimation. The estimation result is shown in Figure 6 with black line. The estimation works well tracking the actual vehicle slip angle in the range of approximately -8 to $+8$ degrees. The estimation cannot track the actual value well if it is out of this range because the friction of the road surface is reduced too much, and in this case the observer gain needs to be recomputed.

If the friction road surface is known, a new observer gain can be obtained. Then, the experiment result of double lane change test on a low friction road surface with the new observer gain is shown in Figure 7 with dash dot red line. The results show that the $\mathcal{H}_\infty$ observer works very well even on the low road friction surface, over the entire range of slip angles from -21 degrees to +10 degrees.

VIII. Conclusions

A new nonlinear observer design technique for vehicle slip angle estimation using inexpensive sensors normally available for yaw stability control applications is developed. The observer design technique utilizes a modified Young's relation and some mathematical manipulation to develop an extended H_∞ circle criterion observer that allows for nonlinear output equations. Additional degrees of freedom are included in the linear matrix inequality (LMI) design condition that make the design less conservative compared to other observer design techniques from literature. The ddeveloped observer is evaluated through experimental tests on a Volvo XC90 sport utility. The experimental results show that the slip angle estimates for a variety of test maneuvers on road surfaces with different friction coefficients are reliable.

IX. Acknowledgments

The research reported in this article was partly supported by a research grant from the US National Science Foundation (NSF Grant CMMI 1562006).

References

[1] National Highway Traffic Safety Administration (NHTSA), "Traffic Safety Facts: Crash Stats," U.S. Department of Transportation, Feb. 2015.

[2] R. Rajamani, *Vehicle Dynamics and Control*. New York: Springer Science & Business Media, 2011.

[3] G. Phanomchoeng, R. Rajamani and D. Piyabongkarn, "Nonlinear Observer for Bounded Jacobian Systems, with Applications to Automotive Slip Angle Estimation", *IEEE Transactions on Automatic Control*, vol. 56, no. 5, pp. 1163-1170, May 2011.

[4] G. Phanomchoeng, and R. Rajamani, "Real-Time Estimation of Rollover Index for Tripped Rollovers with a Novel Unknown Inputs Nonlinear Observer", *IEEE/ASME Transactions on Mechatronics*, vol. 19, no. 2, pp. 743-54, April 2014.

[5] S. Mammar, S. Glaser, and M. Netto, "Time to line crossing for lane departure avoidance: A theoretical study and an experimental setting." *IEEE Transactions on Intelligent Transportation Systems*, 7(2), 226-241.

[6] A. Vahidi and A. Eskandarian, "Research advances in intelligent collision avoidance and adaptive cruise control." *IEEE transactions on intelligent transportation systems*, 4, no. 3 (2003): 143-153.

[7] National Highway Traffic Safety Administration (NHTSA), "Federal Motor Vehicle Safety Standards; Electronic Stability Control Systems," U.S. Department Of Transportation, National Highway Traffic Safety Administration, NHTSA–200727662, 2007.

[8] A. T. van Zanten, "Bosch ESP systems: 5 Years of experience," *SAE Trans.*, vol. 109, no. 7, pp. 428-436, 2000.

[9] A. Zemouche, R. Rajamani, B. Boulkroune, H. Rafaralahy and M. Zasadzinski, "H_∞ Circle Criterion Observer Design for Lipschitz Nonlinear Systems with Enhanced LMI Conditions," in 2016 *American Control Conference* - ACC 2016, Boston, MA, USA, July, 2016.

[10] R. Daily and D. M. Bevly, "The use of GPS for vehicle stability control," *IEEE Trans. Ind. Electron.*, vol. 51, no. 2, pp. 270-277, April 2004.

[11] P. Misra, and P. Enge, *Global Positioning System: Signals, Measurements and Performance*, Second Edition, Massachusetts: Ganga-Jamuna Press, 2006.

[12] D. Piyabongkarn, R. Rajamani, J. Grogg, and J. Lew, "Development and Experimental Evaluation of a Slip Angle Estimator for Vehicle Stability Control," *IEEE Transactions on Control Systems Technology*, vol. 17, no. 1, pp. 78-88, January 2009.

[13] A. Zemouche and M. Boutayeb, "On LMI conditions to design observers for Lipschitz nonlinear systems," Automatica, vol. 49, no. 2, pp. 585-591, 2013.

[14] Y. Wang, R. Madson, and R. Rajamani, "Nonlinear observer design for a magnetic position estimation technique," in *54th IEEE Conference on Decision and Control*, Osaka, Japan, December 15-18, 2015.

[15] A. Zemouche and M. Boutayeb, "A unified $\mathcal{H}_\infty$ adaptive observer synthesis method for a class of systems with both Lipschitz and monotone nonlinearities," Systems & Control Letters, vol. 58, no. 4, pp. 282-288, 2009.

[16] G. Phanomchoeng, R. Rajamani, "Observer Design for Lipschitz Nonlinear Systems Using Riccati Equations", *2010 American Control Conference, Baltimore*, Maryland, USA, 2010.